USING THE RASINTERFOAM CFD MODEL FOR WAVE TRANSFORMATION AND COASTAL MODELING

Gerald C J Morgan[1], Jun Zang[1], Deborah Greaves[2], Andrew Heath[1],
Chris D Whitlow[3] and John R Young[3]

Abstract: The CFD model, rasInterFoam, part of the OpenFOAM library for continuum mechanics, is used to reproduce experimental results for the propagation of monochromatic waves over a submerged bar. The model is shown to reproduce the experimental results very well on the front face and top of the bar, and give adequate results on the back face, even on extremely coarse meshes. Sensitivity analyses are presented for the model results, investigating the dependence on mesh density and discretisation scheme of the model. The modeling of the wave transformations in the model is shown to be broadly insensitive to these parameters within the ranges tested.

Keywords: CFD, OpenFOAM, Wave Propagation, rasInterFoam, Coastal Modeling

INTRODUCTION

Computational fluid dynamics (CFD) is a powerful tools for modeling the behavior of fluids in a wide variety of situations and, with the ever-increasing speed and capability of computer systems, are fast becoming a practical design tool for the assessment of coastal, civil and naval engineering problems. Newer and more accurate design tools are likely to be needed in these areas as sea level rise and climate change begin to affect the assumptions behind the design of many of today's existing sea defences. With this in mind, it is not unreasonable to consider the use of tools such as CFD, which have traditionally been considered too computationally expensive, in the design and assessment of coastal structures.

OpenFOAM is a free, open source library for solving problems in continuum mechanics which has a growing following, both in research and industry. It has built-in support for many of the technical aspects which would have to be considered in the development of a new model, such as parallelism, mesh modification and motion, and turbulence modeling (Weller 1998). At the same time its free licensing model allows it to be used even on small projects where the licensing cost of a commercial package would be prohibitive. The rasInterFoam model examined in this paper has been selected as it is a modern, existing model which is already readily available to designers at no cost through the OpenFOAM project. The version of OpenFOAM used in this paper was 1.5-dev[4].

rasInterFoam is a PISO (Issa 1985) solver for the unsteady, incompressible Navier-Stokes equations with a volume-of-fluid method in which a “volume fraction,” γ, represents the proportion of each computational cell which contains water (Kothe 1999). It can be used with a wide variety of Reynolds-Averaged Navier Stokes (RANS) turbulence models, or simply treat the flow as laminar as was done in the cases described in this paper.

TEST CASE

Beji (1993) performed a series of experiments in which monochromatic, regular waves were generated in a flume and propagated over a submerged bar. These tests were later repeated by Luth (1994) at twice the original scale and these later results are sometimes referred to in the literature as the “Dingemans” test case. It has been widely used for the validation of Boussinesq-type models (see e.g. Gobbi (1999)). This paper recreates these tests using a numerical flume in rasInterFoam.

The Luth experiment was conducted in a wave flume of length 45.0 m with a submerged breakwater as shown in figure 1 and an absorbing beach at the end of the flume. The precise shape of the breakwater is given by the profile in table 1. The water level was recorded at the eleven locations shown in the figure. Three different regular waves were used, referred to as cases A, B and C. The wave parameters are shown in table 2. The results shown in this paper correspond to case A.

[1] Department of Architecture and Civil Engineering, University of Bath, Claverton Down, Bath, BA2 7AY, UK
[2] Centre for Coastal Dynamics and Engineering, University of Plymouth, Room 25, Reynolds, Drake Circus, Plymouth, Devon, PL4 8AA, UK
[3] Edenvale Young Associates Ltd., 12 St. Thomas St. Bristol, BS16JJ, UK
[4] In more recent releases of OpenFOAM, rasInterFoam has been renamed to interFoam.

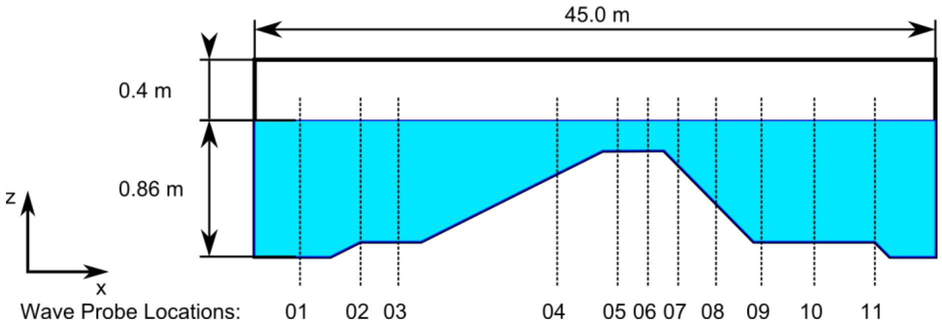

Figure 1. Schematic of the geometry of the "Dingemans" test case showing breakwater shape and positions of wave gauges. Horizontal scale reduced ten times.

Table 1. Bed elevations in meters below mean water level recorded at changes in bed gradient in the "Dingemans" test case.

X (m)	Z (m)
0.00	-0.86
5.22	-0.86
6.42	-0.80
11.01	-0.80
23.04	-0.20
27.04	-0.20
33.07	-0.80
40.61	-0.80
41.82	-0.86

Table 2. Wave parameters used in the "Dingemans" test case.

Case ID	Period, T (s)	Wave Height, H (m)	Wave Length, L (m)	Steepness, H/L, (m/m)
A	2.857	0.04	7.727	0.0052
B	3.571	0.058	9.901	0.0059
C	1.428	0.082	3.012	0.0272

NUMERICAL TESTS

Two issues had to be overcome in the schematization of the numerical flume: correct generation of the incoming wave and the prevention of reflection from the downstream boundary.

New boundary conditions were added to OpenFOAM to allow the generation of an incoming wave based on Stokes' theory. Preliminary testing revealed that for relatively linear, low amplitude waves, the best results were achieved by specifying the volume fraction and horizontal and vertical velocities at the wave inlet boundary faces. For higher, more non-linear waves, it was found that prescribing the volume fraction was not necessary and reduced the overall stability (and hence speed) of the model.

Also considered was a direct simulation of the piston-type wave-maker used in the experiments by using a moving boundary in the numerical flume. This approach was found to be significantly slower, however, as not only did it introduce additional computational workload to handle the moving mesh, but also it required significantly smaller timesteps to resolve the turbulent structures close to the paddle, which are not of interest in this study.

Based on this preliminary work, the wave velocity boundary conditions used in these tests were:

$$U_x(x,z,t) = \frac{gHk}{2\omega}\frac{\cosh(k[d+z-h])}{\cosh(kd)}\cos(kx-\omega t) \qquad (1)$$

$$U_z(x,z,t) = \frac{gHk}{2\omega}\frac{\sinh(k[d+z-h])}{\cosh(kd)}\sin(kx-\omega t) \qquad (2)$$

in which the depth, d, was taken as 0.86, h is the elevation of the mean water level, and x = 0 for this scenario.

The boundary conditions for the volume fraction were calculated using a simple limiting function:

$$\gamma(x,z,t) = \min[\max([\eta'(x,z,t) + h - z], \tfrac{-\Delta z}{2}), \tfrac{\Delta z}{2}] + \Delta z \qquad (3)$$

in which Δz is a small parameter specifying the width of the free surface zone, and η' was given by Stokes' theory:

$$\eta'(x,z,t) = \frac{H}{2}\frac{\cosh(k[d+z-h])}{\cosh(kd)}\cos(kx-\omega t). \qquad (4)$$

OpenFOAM has several options available for modeling wave absorption. Several approaches were tried in preliminary testing including increasing the mesh size to dissipate the waves, modeling a beach as a second structure, and modeling a damping, porous material at the end of the flume. Given the run-times involved in the tests, however, these approaches, which would have further complicated the model were not deemed necessary. Instead, reflection was prevented simply by increasing the length of the numerical flume to 90 m. This was both the simplest and most effective of the available methods and did not increase run times prohibitively.

Meshing was performed using OpenFOAM's blockMesh and snappyHexMesh tools and used the following procedure:

1. A base mesh was generated encompassing the entire flume without any obstruction or breakwater.
2. The cells with their centers within the breakwater were removed from the mesh.
3. The remaining cells were deformed to closely follow the shape of the breakwater surface.

The base mesh allowed 0.4 meters above the water surface to simulate the air movement. Vertical cell sizes were graded so that the cells at the water surface were four times smaller than those at the bed and at the top of the domain. Horizontal cell sizes were graded similarly, with the smallest sizes occurring half way down the rear slope of the breakwater. The base mesh had an average cell size of 0.02 meters in both the horizontal and vertical directions before the insertion of the breakwater.

RESULTS

The results from the model were compared with the experimental data in a number of ways. Graphs showing the modeled water surface elevations (as red, solid lines) compared to the experimental water surface elevations (as green, dashed lines) at each of the wave probe locations shown in figure 1 are presented below.

It can be seen from figure 2 that the modeled results agree well with the experimental results up to and along the top of the breakwater (stations 1 to 7) and the agreement begins to deteriorate slightly for the later results, where the waves become strongly non-linear. The agreement downstream of the breakwater is still very good, however, with the only deviation from the experimental data being in the phase of some of the higher-order harmonics.

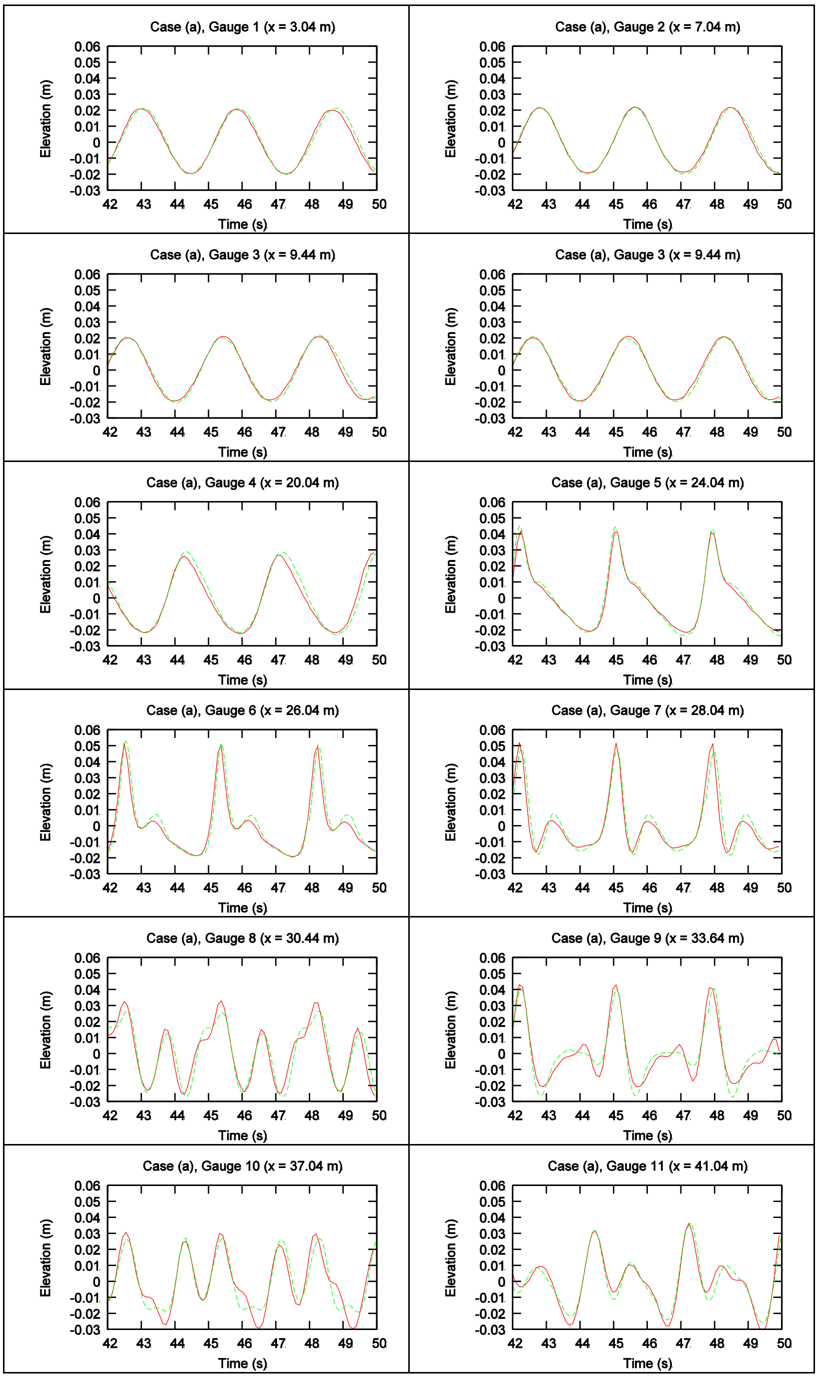

Figure 2. Graphs showing the observed (dashed line) and modelled (solid line) elevation time series at each wave gauge for case A. Note that gauge 3 has two sets of experimental data available.

A similar pattern can be observed if the amplitude frequency spectra are plotted for each wave probe. This has been done in figure 3. These frequency spectra were obtained by trimming the modelled and experimental time series between 33 s and 58 s and applying the Fast Fourier Transform (FFT) algorithm. This window was chosen as it is the time period for which all of the gauges in the experiment experience an undisturbed wave field (i.e. the time from which waves are fully developed at gauge 11 to the point just before the field at gauge 11 becomes contaminated by reflection).

It can be seen that the model correctly represents the frequency of all the major harmonics which are present, and predicts the amplitude of these harmonics to a reasonable degree of accuracy.

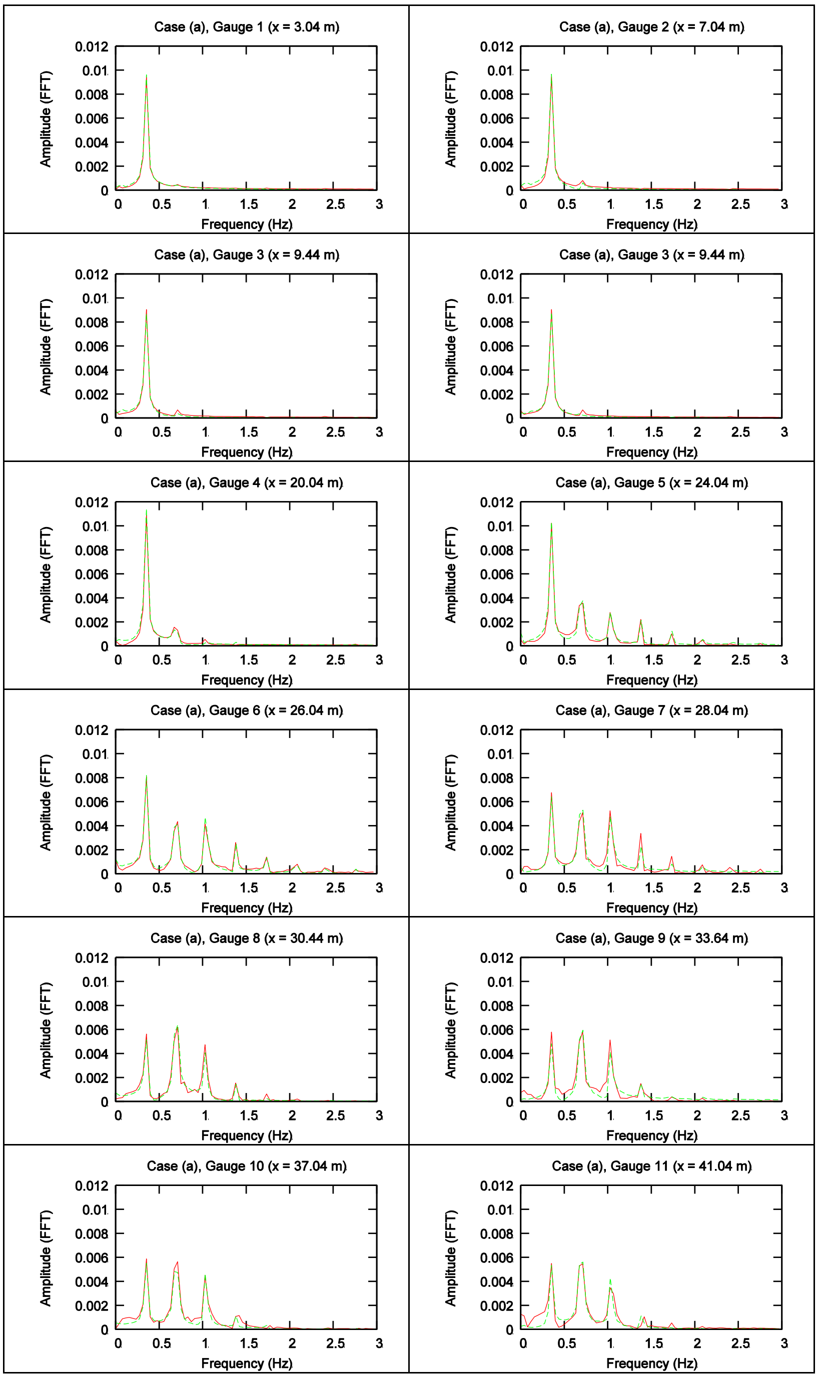

Figure 3. Graphs showing the experimental (dashed line) and modeled (solid line) frequency spectra at each wave gauge for case A. Note that gauge 3 has two sets of experimental data available.

SENSITIVITY ANALYSES

Various sensitivity analyses were performed to investigate the effects of various parameters in the numerical model. The results of these analyses are presented below.

Mesh Size

Four meshes of varying cell sizes were generated using the same procedures as described above. These meshes were labelled from A to D and their parameters are shown in table 3. The baseline results already shown correspond to mesh A. This table also gives an approximate indication of the time taken to run case A on each of these meshes on the specific computer used for these tests. It can be seen that simulations on the coarser mesh A are significantly more efficient than the other meshes. The scale of this effect can be explained not only by the smaller number of cells but also by their greater size: as the timestep of the simulation is controlled by the Courant Number, larger cells lead to larger timesteps and hence faster simulations. Figure 4 shows plots of the cell volume for meshes A, B and C, indicating where the areas of greatest refinement are in these meshes.

Table 3. Mesh parameters used in the sensitivity analysis with the calculation speed for case A in seconds modeled per kilosecond.				
Mesh ID	X size avg. (m)	Z size avg. (m)	Vertical grading	Run Speed (s/ks)
A	0.02	0.02	Yes	70.5
B	0.01	0.01	No	0.583
C	0.01	0.01	Yes	0.648
D	0.005	0.005	No	0.130

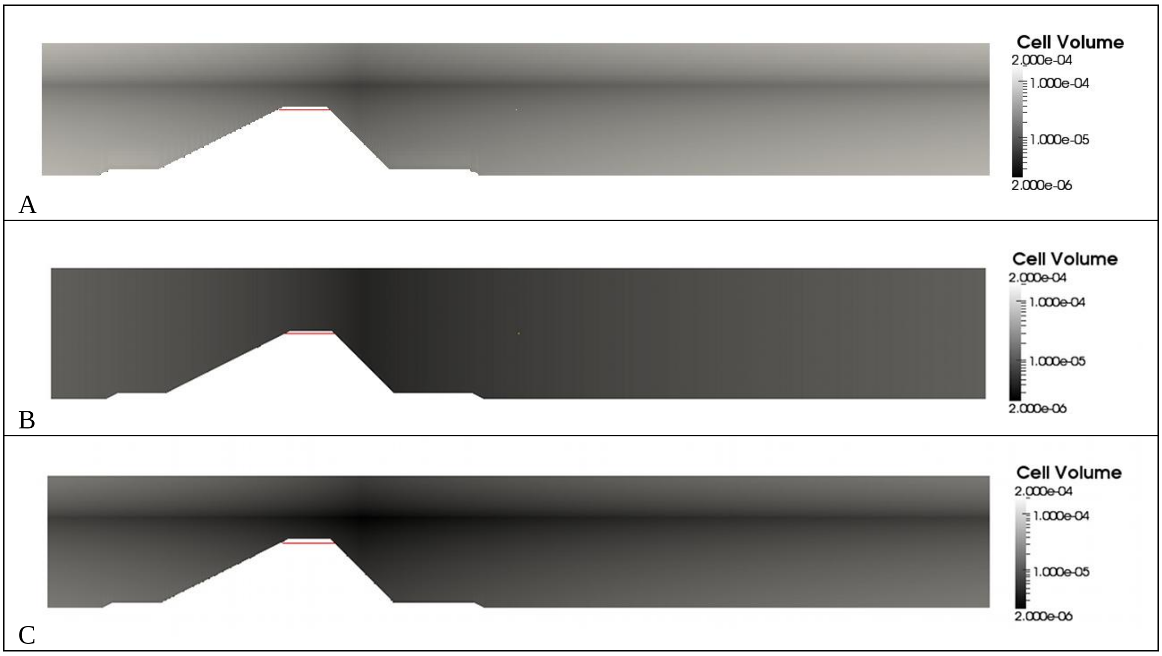

Figure 4. Plots showing cell volumes (in cubic meters) for meshes A, B and C indicating areas of small cell volume (high detail) with darker shading.

Figure 5 shows the results from these sensitivity analyses. It can be seen that the results from mesh A are not appreciably worse than any of the other meshes (with most of the deviations in the mesh D results being attributable to differences in the wave signal). It can also be seen that the results for meshes B and C suffer from slight instability problems in the wave troughs, which may explain the unexpectedly slow speeds of these simulations.

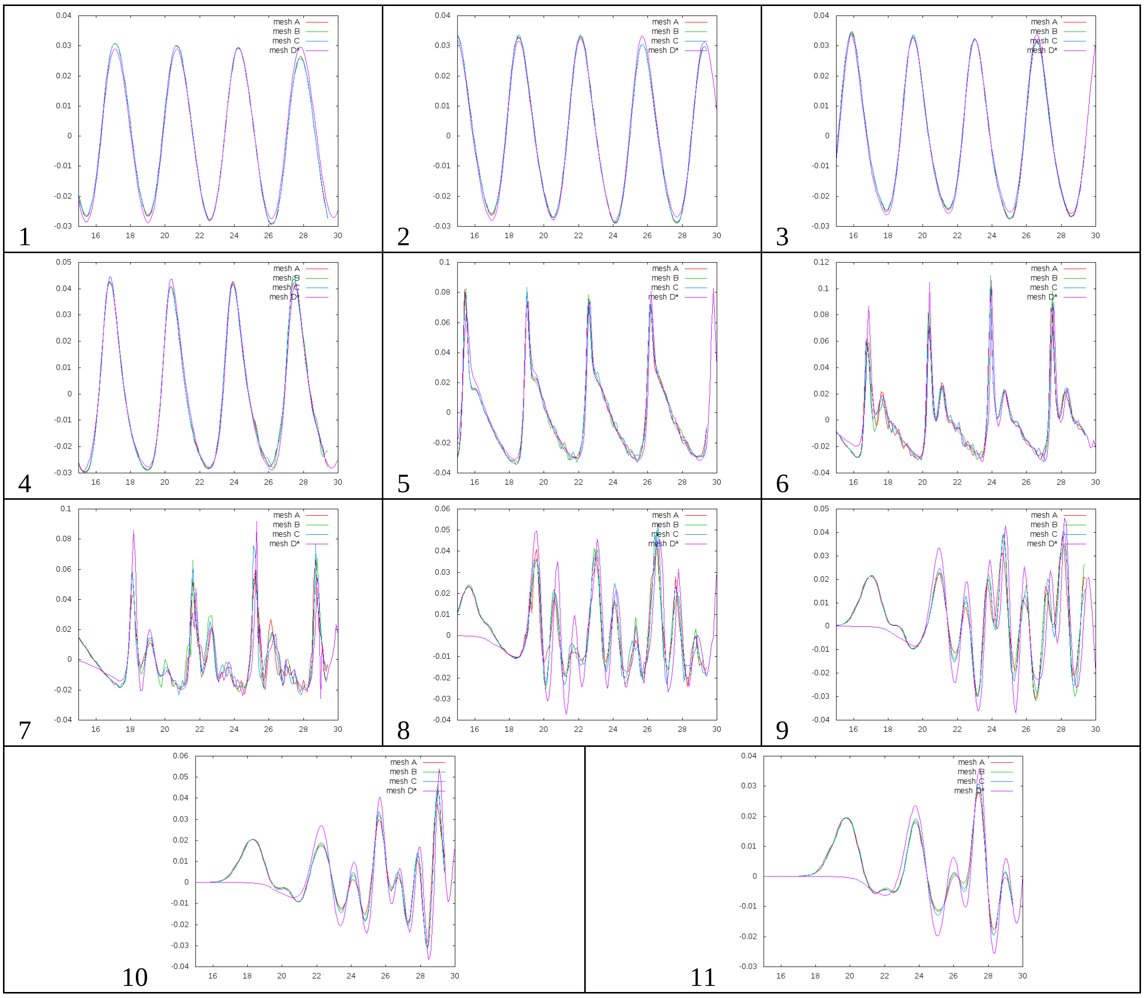

Figure 5. Plots showing the results of case A on four different meshes. Note that the wave signal used for mesh D was inverted (as can be seen on the results from the later wave gauges).

It can be seen that the results for mesh D miss the first peak of the results, which can be seen in the results from the later wave gauges. This is due to the wave signal used for the mesh D results being inverted (i.e. having an initial trough rather than an initial crest). This was shown to have a significant effect on the model results (see figure 6).

Discretization Scheme

Some researchers have suggested that in order to simulate non-linear wave transformations, very high (5th to 9th) order discretization schemes should be used. In order to investigate this, case B was simulated on mesh A using two discretization schemes: a simple linear scheme and a cubic scheme (the very high order schemes are not currently available in OpenFOAM). The results are shown in figure 6. It can be seen that the higher-order scheme does improve the representation of the wave slightly in the troughs, but the improvement is generally minor. Simulations using the cubic scheme required approximately twice the calculation time compared to those using the linear scheme. It should be noted that even higher order schemes might improve the performance of the model in the area after the breakwater. In the figure, the results from the cubic scheme are plotted both with a crest-first and a trough-first wave signal. It can be seen that, at the later gauges, this can have a significant effect.

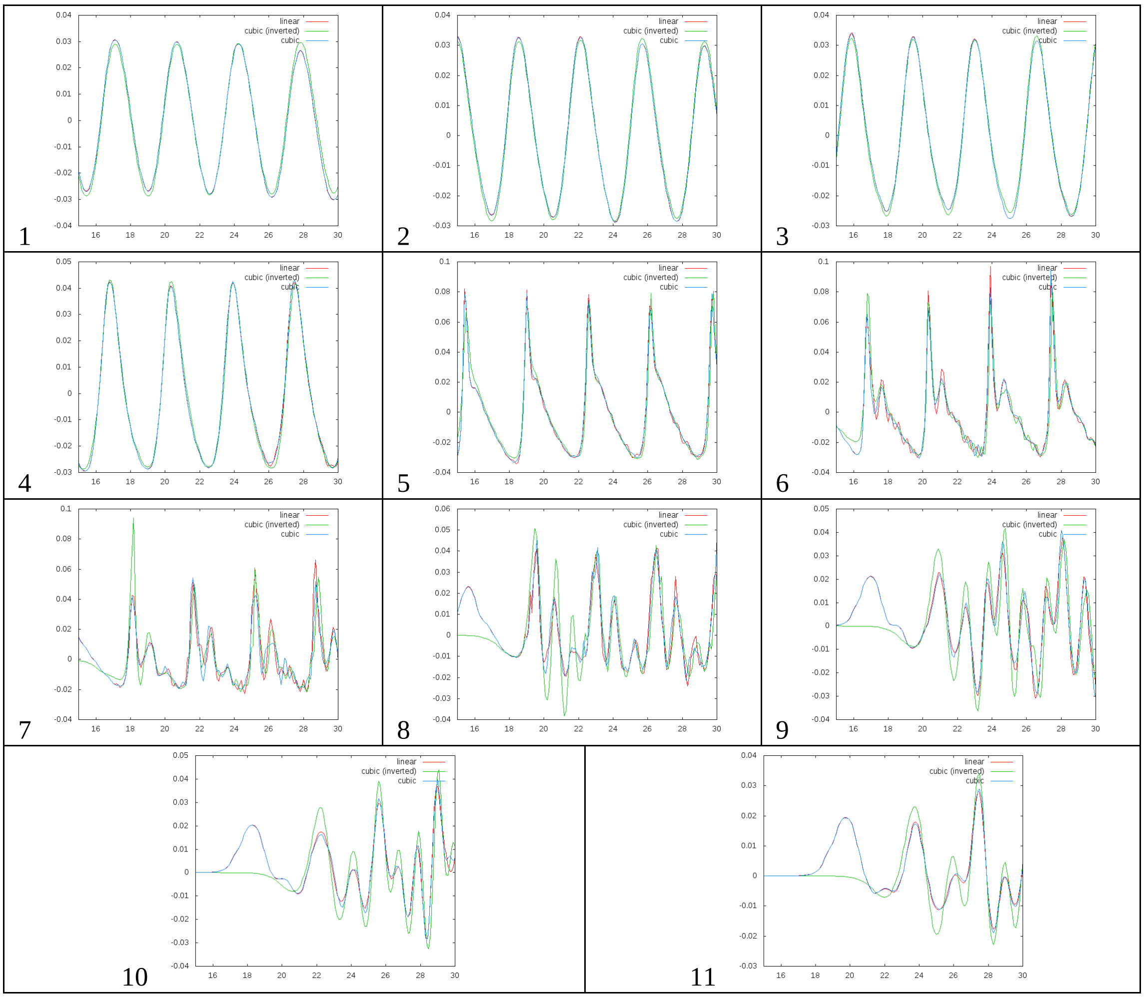

Figure 6. Plots showing the results of case A calculated using linear and cubic discretisation schemes. The cubic discretisation scheme is shown both with the conventional signal and with the signal inverted.

CONCLUSIONS

It has been shown by this study that the rasInterFoam model can simulate and reproduce Beji's (1993) experiments to a reasonable accuracy and that these results can be achieved in a reasonable time and for a comparatively low cost. It has been seen that rasInterFoam performs better on the front face of Beji's embankment than the back and that the accuracy of the model's results decreases with increasing non-linearity of the wave unless the model parameters are carefully selected. From the success of these simulations we can conclude that rasInterFoam could be used to investigate similar problems in practice and might well be suitable for the investigation of coastal defense structures when coupled with a suitable geotechnical model.

The model has been demonstrated to be broadly insensitive to a range of parameters, including the discretisation scheme and the mesh size. This insensitivity to mesh size, in particular, allows future simulations to be undertaken more quickly, using coarser meshes and hence higher timesteps except where very precise results are required.

It has been shown that this problem can be adequately simulated using a linear discretisation scheme, but that some improvement can be seen when a higher-order scheme is used. This suggests that while, for the general case, a linear discretisation scheme is sufficient, higher-order discretisation schemes may be necessary for simulations involving very non-linear waves or more violent interactions.

It can be concluded that OpenFOAM has the potential to be a usable tool for the detailed investigation of wave transformation and wave interaction with structures, and further work should be undertaken to validate its effectiveness for the prediction of forces on coastal and offshore structures.

ACKNOWLEDGMENTS

This work was funded by Great Western Research and Edenvale Young Associates Ltd. whose support is gratefully acknowledged.

REFERENCES

Beji, S. and J. A. Battjes. 1993. Experimental investigation of wave propagation over a bar, *Coastal Engineering*, 19, 151-162.

Gobbi, M. F., and J. T. Kirby. 1999. Wave evolution over submerged sills: tests of a high-order Boussinesq model, *Coastal Engineering*, 37, 57-96.

Issa, R. I. 1985. Solution of the implicitly discretised fluid flow equations by operator splitting, *Journal of Computational Physics*, 62, 40-65.

Kothe, D. B. 1999. Perspective on Eulerian finite volume methods for incompressible interfacial flows, Los Alamos National Laboratory.

Luth, H.R., G. Kloman, and N. Kitou. 1994. Kinematics of wave breaking partially on an offshore bar; LDV measurements of waves with and without a net onshore current, *Delft Hydraulics*.

Weller, J.G., G. Tabor, H. Jasak, and C. Fureby. 1998. A tensorial approach to computational continuum mechanics using object-oriented techniques, Computers in Physics, 12, 620-621.